OPPORTUNITIES FOR JOINT WATER–ENERGY MANAGEMENT

Sensitivity of the 2010 Western U.S. Electricity Grid Operations to Climate Oscillations

N. Voisin, M. Kintner-Meyer, D. Wu, R. Skaggs, T. Fu, T. Zhou, T. Nguyen, and I. Kraucunas

ENSO can be considered to plan for joint water–electricity management to achieve benefits in the western U.S. electricity grid operations, measured by operating cost, carbon emissions, and reliability metrics.

Electric grids must be constantly monitored and managed to ensure that sufficient supply ("generation") is available to meet, or balance, demand ("load") on time scales ranging from microseconds to decades. During typical daily operations, a "reserve margin" of generating capacity that is at least 15% greater than anticipated electricity demand is maintained in order to ensure reliable operations (i.e., ensure that power supply can balance the demand even if there is a loss or reduction in power supply from individual power-generating units)—whether due to maintenance, lack of water, or other disruption. Stress on the grid is typically highest during summer heat waves owing to high building energy demands (for space cooling), sagging electric lines (which increases their resistance and thus hinders their ability to move power through the system), and reduced efficiency of dry cooling thermoelectric power plants resulting in less generating capacity being available to meet demands (Ke at al. 2016). The electric power sector withdraws more surface water than any other sectors in the United States, even though the consumptive use per se remains small (Tidwell et al. 2012; Kenny et al. 2009). Droughts, competing water demands (especially agriculture), and increases in water temperature can all have negative impacts on power production, primarily through reduced hydroelectric generation and wet cooling thermoelectric power production capacity (Harto and Yan 2011; Van Vliet et al. 2016; Bartos and Chester 2015; DeNooyer et al. 2016; Feeley et al. 2008; Sovacool and Sovacool 2009;

AFFILIATIONS: Voisin, Kintner-Meyer, Wu, Skaggs, Fu, Zhou, Nguyen, and Kraucunas—Pacific Northwest National Laboratory, Richland, Washington
CORRESPONDING AUTHOR: Nathalie Voisin, nathalie.voisin@pnnl.gov

The abstract for this article can be found in this issue, following the table of contents.

DOI:10.1175/BAMS-D-16-0253.1

A supplement to this article is available online (10.1175/BAMS-D-16-0253.2)

In final form 15 August 2017

Macknick et al. 2012; Poch et al. 2009). This situation can be of concern when managed water levels are low and a large portion of the generation capacity relies on fresh surface water—which is certainly the case in the western United States, where 67% of capacity depends on fresh surface water (Union of Concerned Scientists 2012). Stress on the grid, and thus the risk of power outages or brownouts due to an inability to deliver sufficient power, is typically highest during summer heat wave events, especially during seasons or years with low water levels.

The North American Reliability Corporation (NERC) has established regulations to avoid the risk of disruptions in power delivery, and the electric power community has developed a wide range of tools to assess grid performance under stress conditions. For example, grid operators perform annual resource adequacy studies under prescribed historically low-water-year conditions to assess generation capacity so that it will meet load even under the worst drought conditions (e.g., Poch et al. 2009; Macknick et al. 2012). These adequacy studies utilize data surveys (observed water withdrawals per generator, etc.), sometimes combined with hydrology simulations, to assess how low-water conditions could reduce hydropower generation as well as the capacity of thermoelectric plants as a result of constrained withdrawals (Macknick et al. 2012; Tidwell et al. 2012; Poch et al. 2009; Boehlert et al. 2016; Kao et al. 2015). Forward-looking analyses and modeling of the energy–water nexus is an emerging area of research. For example, Tidwell et al. (2016) combined water withdrawal estimates and simulated natural flow at thermoelectric power plants to understand how grid expansion could affect grid stress under current and future flow conditions. Remaining challenges in power system modeling research (e.g., representation of hydrothermal coordination, energy markets, and grid expansion simulations) include accounting for errors in simulated water availability and ensuring the consistency of streamflow information for thermoelectric and hydropower plants.

Several recent studies, including Van Vliet et al. (2016), Bartos and Chester (2015), and Harto and Yan (2011), have attempted to assess the potential impact of changes in water availability on both hydropower generation and thermoelectric plant capacity by using a macroscale hydrology model forced with observed and projected meteorological forcing. Although these studies provide insight into how future changes in precipitation and temperature could potentially affect water-dependent electricity generation, they do not attempt to resolve the operations of the electricity system explicitly.

These and other studies have increased our appreciation of the potential influence of changes in water availability on power production but have not attempted to simulate the actual impact of water scarcity—regardless of its origin—on the reliable operations of regional electric grids. To better understand the true vulnerability of the electric grid to changes in water availability, it is important to simultaneously simulate electricity and water system operations, and particularly during hot and dry conditions when grid stress is typically most acute.

Voisin et al. (2016) directly linked integrated hydrology simulations with a unit commitment and economic dispatch (UCED) model. UCED models are power system models that simulate the operation of a fleet of electricity generators, typically at hourly resolution subject to certain boundary conditions and operating constraints, in order to simulate the costs of meeting electricity demand, reserve margins, and related variables such as greenhouse gas emissions. Voisin et al. (2016) used a UCED model in which both potential hydropower generation and thermoelectric capacity at individual plants are adjusted according to changes in simulated regulated flows. This 2016 proof-of-concept study demonstrated how droughts in the western United States, which is highly dependent on freshwater for power production, could impact the ancillary services (set of power operations to maintain grid reliability). The results also suggested that information on regional variability in water availability, especially between California and the Pacific Northwest (PNW), could potentially improve western U.S. power operations. The large spatial extent of the western grid, combined with the prevalence of several strong modes of interannual climate variability and water availability, raises the possibility of strong spatiotemporal patterns in the coupled regional energy–water system (Cayan et al. 2003). For example, El Niño–Southern Oscillation (ENSO) (Trenberth 1997) has a bimodal pattern in the PNW and California and a moving boundary in Northern California (Dettinger et al. 1998). This bimodal climate pattern has already shown potential to require higher north–south power transfers during La Niña events (Voisin et al. 2006). Another notable regional variability pattern is the Pacific decadal oscillation (PDO; Mantua et al. 1997), which has been shown to modulate ENSO effects on water availability and potential hydropower generation (e.g., Hamlet and Lettenmaier 1999). It may be important to account for multiple modes of variability because ENSO tends to shift phase every 12–18 months, while the PDO has a decadal phase, and the combined effects of these two oscillations could potentially lead to multiyear droughts (e.g., Wang et al. 2014).

In the current paper, we extend the Voisin et al. (2016) study to investigate how interannual climate oscillations, especially the ENSO and PDO, could support joint water–energy management planning. We use a 55-yr-long historical observed gridded weather dataset and 2010 level of water demands to force an integrated water model. Regulated flow at hydropower plants and fresh surface water–dependent thermoelectric plants is translated into boundary conditions for a UCED model representing 2010 level of western U.S. grid operations. We do not attempt to reproduce historical grid operations because the electricity grid infrastructure, load, and generation portfolio have changed markedly over the last decades. Rather, our focus is on understanding the sensitivity of the western U.S. grid as it existed in 2010 to historical climate oscillations. In addition to serving as a benchmark of system performance, these results are useful for seasonal and multiyear planning of joint energy–water management and can be used to support regional impact, adaptation, and vulnerability analyses.

We address the following science questions in this paper:

- What is the range of grid operations in the western U.S. grid in August, when generation is typically most constrained by water availability and energy demand and grid stress is typically highest?
- What is the sensitivity of grid operations to regional variability in seasonal water availability associated with the dominant large-scale climate oscillations in the region (i.e., ENSO and PDO)?

The next section introduces the analysis domain, datasets, and integrated water–energy modeling framework. Then, we present how we designed the analysis to capture the cascade of climate teleconnection signals from water availability onto power system operations. Finally, our results are presented and discussed.

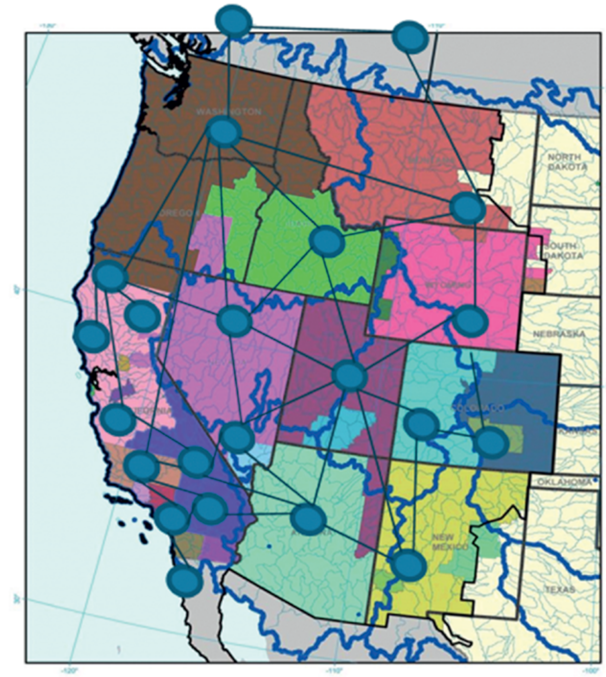

Fig. 1. Representation of the 22 load zones in the western grid (green circles, colored regions) and the possible transfer paths between them. Hydrologic regions are delineated in blue (Voisin et al. 2016).

DOMAIN, MODELING FRAMEWORK, AND DATASETS. The western grid spans most of the United States west of the Mississippi River (Fig. 1). The Western Electricity Coordination Council (WECC) is responsible for grid reliability across this domain, so it is often referred to as the WECC interconnection or WECC grid. Within the WECC grid are 22 generation/load zones, which are often the basis for UCED modeling. The WECC region includes all or parts of seven U.S. hydrologic regions: the PNW (i.e., Columbia River basin and coastal areas), California (San Joaquin–Sacramento and coastal areas), Great Basin, Colorado River basin, upper Missouri River basin, upper Arkansas–Red River basin, and upper Rio Grande basin. Note that results for water availability are presented by hydrologic regions whereas grid performance metrics are presented by energy regions, mostly WECC-wide, but also for the California and PNW zones for selected results.

We leverage the overall Voisin et al. (2016) modeling framework, which translates hydrology simulations into boundary conditions anomalies for UCED models, therefore addressing the hydropower–thermoelectric plant dependencies as well as flow errors. The section presents the integrated modeling framework and in particular the water modeling, the power system modeling, and then the coupling.

Integrated water modeling framework. The 1956–2010 water availability, which affects water-dependent electricity generation throughout the WECC region, is simulated using a combination of hydrology, river routing, water management, and integrated assessment models. Gridded daily hydrologic simulations for 1950–2010 are based on the Variable Infiltration Capacity (VIC) hydrology model (Liang et al. 1994) and gridded-observation dataset (Maurer et al. 2002; Livneh et al. 2013) and were obtained from the World Climate Research Programme (WCRP) phase 5 of the Coupled Model Intercomparison Project (CMIP5; Taylor et al. 2012) website. These natural flow simulations were evaluated by the Bureau of Reclamation (2014, 2016). To simulate the effects of river routing and reservoir operations, the daily spatially distributed runoff and base flow from Livneh et al. (2013) were used to drive a coupled river routing and water resources management model, namely, the Model for Scale Adaptive River Transport (MOSART; Li et al. 2013) and water management (WM; Voisin et al. 2013a) model. MOSART-WM simulates the effects of reservoir regulations (i.e., for flood control, irrigation, and minimum environmental flows) and withdrawal operations on the river system and outputs regulated flow. Similar to a hydrology model that needs to be run for a couple years for water storage to reach equilibrium and be representative, the storage in the reservoir model is initialized at 90% full and needs to reach equilibrium for seasonal and interannual storage variations and regulated flow simulations to be meaningful. Reservoirs whose capacity is smaller than the annual inflow will reach equilibrium in less than a year while large storage reservoirs managed for multiple years will need a couple years. Thus, 5 years (January 1950–October 1955) are used as a spinup of MOSART-WM in order to reach equilibrium given that we simulate that the western United States and reservoirs over the Colorado River basin can store up to 4 years of annual flow. The 2010-level gridded water demand is provided by the Global Change Assessment Model (GCAM) (Davies et al. 2013; Hejazi et al. 2013, 2014a,b), which is calibrated with respect to reported 2005 U.S. Geological Survey (USGS) withdrawals (Kenny et al. 2009). Voisin et al. (2013b), Hejazi et al. (2015), and Scott et al. (2016) report previous applications of this integrated water modeling framework.

Power system modeling. The role of a balancing authority is to balance out electricity demand with supply. Figure 1 shows a simplified representation of the WECC in 2010 with 33 balancing authorities aggregated into 22 load-zone regions (green circles). Hourly demands are specified for each load zone. The zonal production cost model (PCM) PROMOD IV is a security-constrained UCED model that represents transient power system operations over all hours of a year, not just peak hours over specific seasons (as is typically done in grid expansion models). PROMOD optimizes the hourly generation of electricity based on a portfolio of technology (hydropower, thermoelectric, wind, solar, nuclear, combustion turbines) and asset characteristics (cost, capacity, minimum generation, type of contracts, etc.) to meet hourly loads in each zone for the lowest cost. The model then optimizes transfer between zones, equivalent to transmission systems. Each load zone is assumed to have no congestion of electricity transfers within its boundary. Congestion can only occur in the transfers from one zone to the other. This assumption is standard when using zonal electricity models instead of nodal representations (i.e., substation level). Different electricity models specifically focus on distribution. The model runs for 1 year at a time. Input into the model includes 2010 observed electricity demand [obtained from Allmänna Svenska Elektriska Aktiebolaget (ASEA) Brown Boveri (ABB)] and boundary conditions in electricity generation, for example, monthly potential hydropower generation and thermoelectric generation capacity at individual power plants. The baseline boundaries are set for the 2010 water year, which was close to an average water year over the WECC domain (43rd percentile out of the 1956–2010 hydrology climatology presented in the "Integrated water modeling framework" section). The baseline boundary conditions, hourly load, and grid infrastructure (power plants, generation portfolio and constraints, transmission capacities) were obtained for 2010 from Ventyx (now ABB). Key outputs of PROMOD include economic metrics such as the cost of power operations (i.e., "production cost") and reliability metrics such as reserve margin or "unserved energy," which tracks when the balancing of the energy demand might need alternative operations, such as curtailment, to avoid brownouts or power outages. It also includes the generation of electricity by technology sources and corresponding sustainability metrics such as carbon emissions.

Linking hydrology simulations to grid operations modeling: The boundary conditions. When assessing water resources changes, simulated natural flow is usually bias corrected before forcing operational water management models (e.g., Bureau of Reclamation 2016). Understanding simulation errors in integrated water modeling (i.e., regulated flow, stream temperature, and the development of associated postprocessing for application in sectoral models) is an area of future research. In our approach, hydropower generation and thermoelectric capacity are not directly estimated by using the reservoir models or by looking at water availability and stream temperature constraints. Instead, we rescale the baseline boundary conditions, that is, the 2010 hydropower potential generation obtained from the electricity model database used as a reference. For each hydrologic region, for all hydropower plants, the relative departure from the annual regulated flow from the 2010 reference, weighted by the plant generating capacity, is used to derive a regional adjustment. The regional adjustment is used as an energy constraint, or boundary condition, for the potential hydropower generation in the production cost model (Voisin et al. 2016). The potential hydropower generation at each power plant is adjusted with respect to 2010 annual regulated flow. For thermoelectric plants, the same approach is used but the adjustment at each plant is limited to 100%. The maximum generating capacity is assigned for the water availability condition in 2010. Thermoelectric capacity is derated less than 43% of the years in the 55-yr-long simulation. The adjustment and derating are further detailed in Voisin et al. (2016) and discussed in the first section of the online supplemental material (https://doi.org/10.1175/BAMS-D-16-0253.2).

The product is a time series of potential hydropower generation boundary conditions at each plant, which differs from actual hydropower generation provided by other studies. Potential hydropower is to provide different types of services to the grid including capacity reserve, renewable balancing, and firm generation. The output of PCM includes the optimized hydropower generation to be used for our analysis. The time series of derated thermoelectric plant capacity is consistent in space and time with the potential hydropower boundary conditions, which is strategic for the PCM optimization (e.g., the hydrothermal coordination) and which will affect the PCM estimated hydropower generation, production cost, and carbon emissions. The sensitivity of different PCM optimization approaches to boundary conditions is the subject of future research.

ANALYSIS APPROACH. We analyze the sensitivity of water availability metrics specific to electricity infrastructure to climate teleconnections and cascade it into power operations (i.e., PROMOD output).

2010-grid operations sensitivity to historical water availability. A dataset of 55 years of monthly water availability was derived using the integrated water modeling framework described in the "Integrated water modeling framework" section, further translated into 55 years of generation and capacity boundary conditions for hydropower and thermoelectric generators in the western grid and input into PROMOD. Energy electricity loads usually peak during July and August. August and September are typically the months with the lowest water availability (Schaner et al. 2012), which affects water-dependent electricity generation (Van Vliet et al. 2012a). We therefore choose to focus on August grid operations during the 55 years of simulation in order to combine high electricity demand with water-constrained generation conditions. The planning reliability metric unserved energy was used. It indicates the energy demand that could not be balanced under normal operations (i.e., without curtailment or load-shaving, for example, or use of alternate sources of water) under specific hydroclimatological conditions. In operations, contingency plans allow deviations from normal operations in order to ensure reliability of supply. Contingency plans are not evaluated, although the approach could inform an optimal design of contingency plans. Another reliability metric, planning reserve margin, was used, which is defined as the percentage of the available capacity in excess of the peak demand. NERC suggests a planning reserve margin of 15% above estimated peak load. Economic metrics include the total production cost for serving all WECC customers, which estimates the economic implications of the varying availability of water-dependent resources. This metric reflects the total value of water from an electricity generation perspective. Another metric is the carbon emissions associated with the generation of electricity. With sufficient water availability, zero-emitting hydropower can displace natural gas and coal-fired generation and, thus, reduce total carbon emissions. Potential changes in biogenic emissions from hydropower are not represented in this framework.

Gridcentric drought severity index. Voisin et al. (2016) demonstrated the interdependencies between water availability and grid operations and introduced the water scarcity grid impact factor (WSGIF). The WSGIF is a new index quantifying the severity of a drought from the perspective of grid operations. It combines the deviation of the annual regulated flow from the long-term mean annual flow (1956–2010 in this study) at each water-dependent power plant (hydropower and thermoelectric) and weights the deviation by the plant's generating capacity. The regional hydropower and thermoelectric adjustments are combined (simple addition) into the WSGIF, which therefore theoretically varies from 0 to about 4. Low values indicate severe droughts, median values tend to be around 1.9 to 2, and wet years are above the value of 2. WSGIF can be computed at the WECC-wide scale and at the scale of the two-digit hydrological unit code (HUC2) regions. There is high regional variability in WSGIF, and California displays the largest range in interannual variability. This simple metric allows combining the impacts of water scarcity on both hydropower (flow) and thermoelectric plants (constraints on withdrawals) in space and time with a consistent bias correction in hydrology simulations. The metric could be further refined with more complex information on thermoelectric derating in particular. Weights could also be customized for other electricity grids where the role of hydropower and hydrothermal coordination might not be as important as over the western United States.

The WSGIF has previously been shown to be linked to grid operations metrics (Voisin et al. 2006) and allows the definition of the system resilience or robustness to be linked to water availability. The WSGIF-based system performance threshold indicates the WSGIF conditions for which some loads are not served—quantified as unserved energy—because the zonal generation capacity or transfer capability is insufficient. Here, the full set of grid operation metrics (unserved energy, reserve margin, carbon emissions, and production cost increases) are linked with their associated historical WSGIF.

The seasonal predictability of the summer grid operations is evaluated by assessing the explained variance in grid performance metrics through the WSGIF given that over the western United States, the WSGIF should be fairly accurate by 1 April on the onset of snowmelt.

Long-term operations—Sensitivity to climate oscillations. We hypothesize that grid operations should be sensitive to both ENSO and ENSO combined with PDO conditions because these modes of climate variability have been shown to drive interannual variability in water resources over the western United States (Redmond and Koch 1991; Hamlet and Lettenmaier 1999). We evaluate how regional and WECC-wide WSGIF are sensitive to ENSO conditions. We then explore the sensitivity of the grid operations performance metrics based on ENSO and PDO large-scale climate oscillations and discuss the cascade from ENSO to WSGIF to grid metrics.

The oceanic Niño index (ONI) (Barnston and Ropelewski 1992) was obtained from the NOAA Climate Prediction Center (www.cpc.ncep.noaa.gov/products/analysis_monitoring/ensostuff/ensoyears.shtml). It is used to define positive (El Niño) and negative (La Niña) phases when anomalies are higher or lower than +0.5 and −0.5, respectively. In our 55-year dataset we isolated 8 positive and 11 negative ENSO years, with the remainder classified as "neutral." Digital values of the PDO index (Mantua et al. 1997) were obtained online (http://research.jisao.washington.edu/pdo/PDO.latest). Similarly, we find 20 years with a positive PDO index and 35 years with negative PDO, respectively. Out of 11 La Niña years, 9 years are compounded with negative phases of PDO; 6 out of 8 El Niño years are compounded with positive phases of the PDO.

RESULTS. *Validation of the integrated water modeling framework.* The Bureau of Reclamation (2014) natural flow simulations are implemented in the integrated modeling framework (see "Power system modeling" section); that is, they force the river routing

Table 1. Simulated regulated flow performance with respect to observed regulated flow.

	Natural flow: Correlation	Change in correlation when including WM	Natural flow: rmse (cm)	Change in rmse when including WM	Natural flow: Relative bias	Change in relative bias when including WM
Sacramento River at Bend Bridge, Red Bluff, CA	0.530	1%	373	−15%	−2%	−13%
Columbia River at The Dalles, OR	0.453	8%	2,905	−41%	−16%	−4%
Missouri River at Hermann, MO	0.331	12%	1,886	−21%	26%	28%
Rio Grande at Albuquerque, NM	0.231	−54%	135	21%	113%	77%
Arkansas River at Ralston, OK	0.177	−35%	282	−15%	−15%	25%
Texas–Gulf: Neches River at Diboll, TX	0.163	−1%	52	−18%	0%	−3%
Great Basin: Humbolt River at Imlay, NV	0.147	−5%	54	−10%	−74%	3%
Colorado River at Imperial Dam (CA–AZ border)	0.099	−55%	377	−47%	−39%	−8%

water management model. Typically, in a nodal architecture water management model used operationally such as RiverWare (Zagona et al. 2001), runoff is routed into entry point and bias corrected because reservoir operations based on thresholds and specific flow and storage targets are not consistent with uncorrected flow (Vano et al. 2010). In this spatially distributed large-scale water management modeling framework, flow is not corrected upon entry into reservoirs, and therefore operations need to accommodate for errors in flow simulations and yet still mimic overall river operations (Voisin et al. 2013a). Natural flow simulations were evaluated by the Bureau of Reclamation (2014). Thus, we evaluated here how the water management model modifies the natural flow and how this modification is representative of the observed operations. Table 1 presents monthly performance statistics of the simulated regulated flow with respect to observed regulated flow over the 1997–2007 period. Each metric [correlation, root-mean-square error (rmse), and relative bias] is associated with the corresponding change from what the metric would be if the Bureau of Reclamation (2016) natural flow simulations were used. The change indicates the contribution of the large-scale water management model representation to the metric. The monthly rmse is the most improved metric when representing large-scale water management. The integrated water availability simulations are similar in performance to those obtained using other large-scale integrated analyses (Van Vliet et al. 2012b; Biemans et al. 2011; Döll et al. 2009; Hanasaki et al. 2006). Annual flow is used for the computation of the generation and capacity adjustments and the WSGIFs.

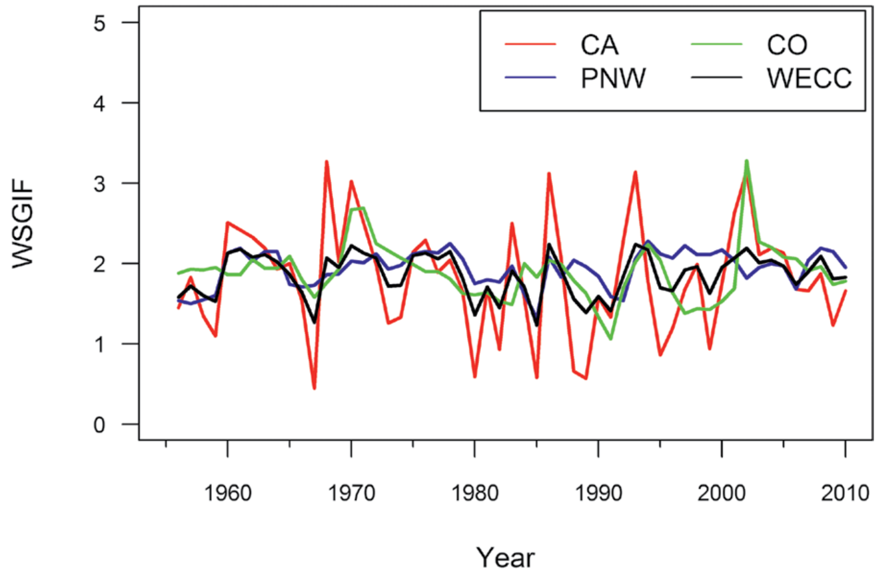

Fig. 2. The 1956–2010 time series regional WSGIF for the California (CA), Colorado (CO), and PNW hydrologic regions and the WECC energy region.

55 years of boundary conditions reflected in the WSGIF. Figure 2 presents the time series of the annual WECC and regional WSGIF over the 1956–2010 period. It presents the overall degree and sequencing of interannual variability for the different regions and highlights the in-phase and out-of-phase regions. California has the largest interannual variability. Note in particular a couple periods of high WSGIF interannual variability with low WECC-wide and low California WSGIF values: 1967, the 1980s, and 1999. Those years differ from other outstanding dry years in California as defined by the standardized precipitation index (SPI; McKee et al. 1993) and Palmer index (Palmer 1965) based on physiographically sensitive mapping of climatological and precipitation [Parameter-Elevation Regressions on Independent Slopes Model (PRISM)] data (Daly et al. 2008), because of the weighting of the hydrologic streamflow at specific places in the WSGIF computation, in addition to integrated modeling uncertainties (see "Planning of grid operations" section in the supplement).

Boundary conditions under ENSO and PDO conditions. Using a regression analysis of the annual-time-series WSGIF with ENSO and PDO indices, Table 2 shows the explained variance of the WECC-wide and regional WSGIF using the climate indices. As seen in the table, 37.4% of the WECC-wide WSGIF variance can be explained by the PDO index, while 23.6% can be explained by the ENSO index. It tends to indicate that both PDO and ENSO indices can be useful to

Table 2. Percentages of WECC and regional WSGIF variance explained by ENSO and PDO.

	ENSO	PDO
WECC-wide WSGIF	23.6	37.4
California WSGIF	23.5	32.0
PNW WSGIF	35.6	19.3

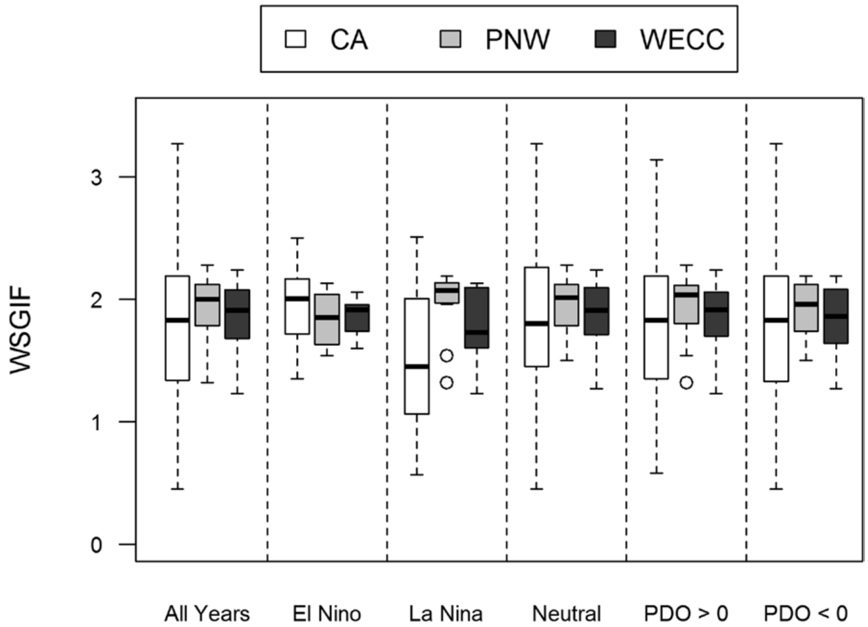

Fig. 3. Regional WSGIF by ENSO and PDO phases.

predict WSGIF ahead of time and therefore the summer grid operations metrics.

Figure 3 shows the range of WSGIF for all years and specific years corresponding to ENSO and PDO phases for WSGIF in order to assess the median impact of those large-scale oscillations. WSGIF tends to be lower (droughts) in California during La Niña years and higher during El Niño years, which is consistent with hydroclimatology literature (Redmond and Koch 1991). The range of WSGIF also tends to be narrower during those years, which might support decision-making. The interannual variability over the PNW is much lower than over California. There is a good correlation between ENSO and WSGIF over the PNW (Table 2; 35.6% variance explained), and WSGIF tends to be drier (lower) during an El Niño year and wetter during positive phases of the PDO. At the WECC scale, the WSGIF tends to be lower during a La Niña event but with large uncertainty. During an El Niño the WECC WSGIF tends to be slightly drier, but the uncertainty is much lower with a reduced ensemble size. Even though the correlation with PDO at the WECC scale and regionally is relatively high, there is little resolution in projecting WSGIF based on the PDO index: the medians are about the same and the uncertainty remains similar to the whole climatology sample.

55 years of 2010-level grid operations. Grid impacts are assessed by four metrics: 1) unserved energy, 2) planning reserve margin, 3) total production cost for generation and delivery of electricity, and 4) carbon dioxide emissions from generation plants. Figure 4 represents the metrics based on a 2010 grid infrastructure for exposure to 55 years of water availability conditions.

Figure 4a represents the total available electricity generation capacity, which was adjusted according to the WSGIF. Significant reduction in the available capacity of up to 15% can be observed. The WECC-wide 2010-level generation capacity would have been challenged during the 1980s (1980, 1982, 1985, 1988, and 1989), and then over specific years like 1959, 1967, 1995, 1996, and 1999, based on water availability.

Figure 4b shows the percentage of unserved energy for the month of August. During the 55-yr period, 5 years (1967, 1980, 1985, 1988, and 1989) would have seen significant unserved energy over the month of August under normal operations. Figure 4c shows the reserve margin (i.e., the planning reserve capacity). The minimum reserve requirement of 15% from NERC would not have been violated during any years that had a minimum reserve of 20%, even for the 5 years with unserved energy. It indicates the difference in the reserve margins definition between planning (sufficient capacity) and operations margin (unserved energy). While sufficient installed capacity may be in the system, when operating under conditions of low water availability, online resources may be unavailable or insufficient. This difference in definition further motivates to complement resource adequacy studies with the use of a PCM.

Figure 4d shows the production cost for the month of August. The trajectory is very similar to that of unserved energy caused by a price penalty in the PCM whenever the system does not meet its obligation to serve all customers. The annual variations tend to vary from –10% to +50% of the August 2010 baseline ($1,969,000) before there is unserved energy. Estimates when there is unserved energy are not used because they are linked to the price penalty in the formulation of the PCM optimization and do not reflect the cost of contingency operations.

Figure 4e shows carbon dioxide emissions from the production of electricity. Understanding the interannual variation and dependence of electricity-related

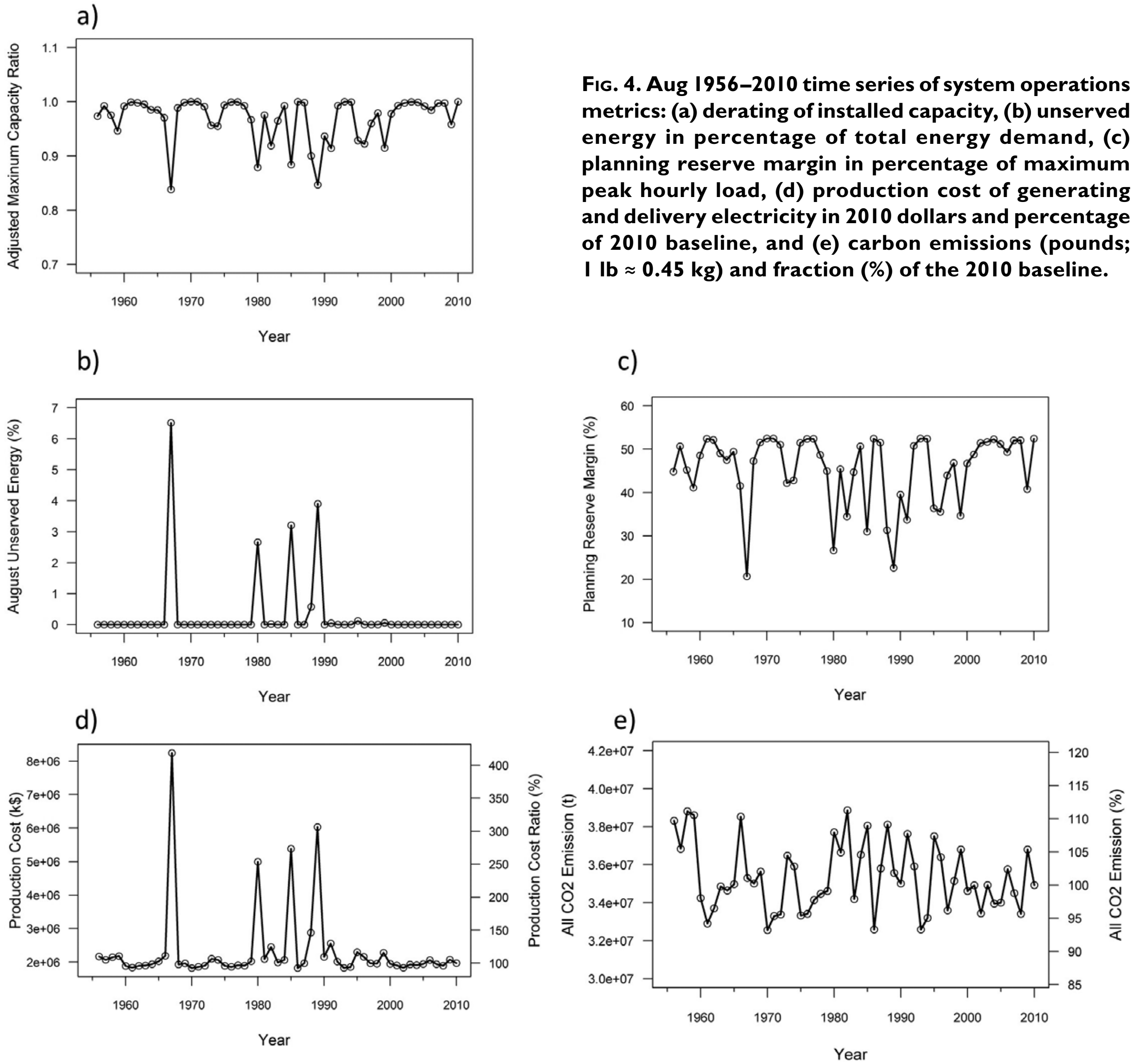

Fig. 4. Aug 1956–2010 time series of system operations metrics: (a) derating of installed capacity, (b) unserved energy in percentage of total energy demand, (c) planning reserve margin in percentage of maximum peak hourly load, (d) production cost of generating and delivery electricity in 2010 dollars and percentage of 2010 baseline, and (e) carbon emissions (pounds; 1 lb ≈ 0.45 kg) and fraction (%) of the 2010 baseline.

carbon emission as a function of water availability can inform future integrated modeling for adaptation studies to meet carbon emissions targets. The 2010 level of carbon emission is considered the reference. The time series indicate low emissions during years of higher water availability as hydropower replaces fossil generation. This trend can be observed in the 1960s and 1970s. Interannual variability in carbon emissions ranges from –7% to +10% around the 2010 baseline.

Sensitivity of operations to ENSO conditions. Estimates of power operations under ENSO phases below are based on the relative median departure of the grid performance metric in each ENSO phase with respect to the long-term (55 yr) median.

The hydropower generation metric (Fig. 5a) combines the potential impact (WSGIF) into large-scale power system operations. It is a function of available potential hydropower generation (WSGIF) and desired ancillary services by the PCM optimization. At the WECC scale, hydropower generation tends to decrease under both ENSO phases (–3% and –4% under negative and positive phases, respectively), which indicates that neutral ENSO years are more beneficial at the WECC scale (1%). The use of PDO provides little resolution for projecting hydropower generation over the WECC. In California, hydropower generation tends to be –17%, –1%, and +14% with respect to the long-term average under negative, neutral, and positive ENSO phases, respectively. The PNW has 6%, 1%, and –7% deviations in contrast. Those results are consistent with the regional

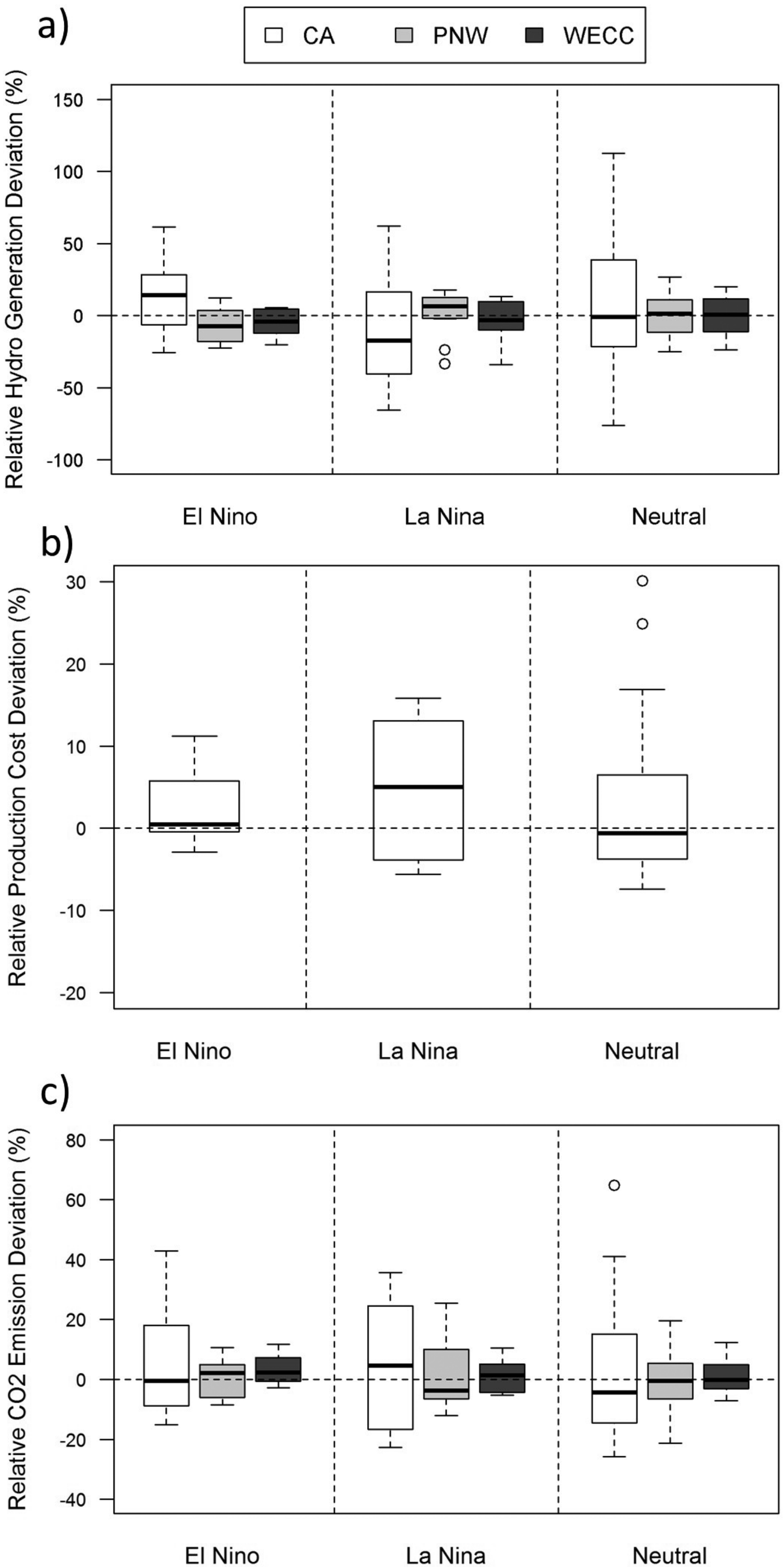

Fig. 5. Range of Aug median deviation in hydropower generation, Aug median deviation in production cost deviation, and Aug median deviation in carbon emission from the climatology (1956–2010 median) when under different ENSO conditions.

water availability sensitivity to ENSO phases.

Three out of the five events with unserved energy occurred during neutral ENSO years and the other two during La Niña conditions. The PDO index provides little resolution; there are about as many unserved energy events distributed over the two phases.

Figure 5b presents the range of August production costs for years without unserved energy. The production costs during La Niña (+5%) and El Niño events (0%) tend to be larger than during neutral conditions (–1%). This condition seems to be related to the stronger distribution diversity of water across the regions, which affects the production cost because the balancing authorities first need to use all of their capacity before importing more through the transmission system. Although beyond the scope of this analysis, a regional analysis of power operations would give more insight.

Figure 5c presents the range of carbon emissions, which tend to be higher at the WECC scale under both El Niño (2%) and La Niña (2%) than under neutral conditions (1%). The regional carbon emission deviation is linked to the regional hydropower generation, with higher emissions in California (+5%) and lower emissions in the PNW (–4%) under La Niña conditions. This finding reinforces the analysis that El Niño and La Niña years are more challenging for western U.S. grid operations. Lowest carbon emissions in California are expected under neutral conditions (–4%). Compounding PDO over ENSO conditions tends to not change drastically the results owing to the small size of the sample.

Uncertainties. The first section of the online supplement discusses the advantages of the WSGIF index with respect to non-sector-specific drought monitors for application to the energy sector. The second section of the supplement discusses the derating of thermoelectric generation capacity and hydropower generation and indicates that our adjustment estimates are within the range of other studies. The third section of the supplement highlights the value of using a PCM to quantify the impact of changes in water availability on power operations and complement existing literature on the potential impact. The fourth section of the supplement further quantifies the relationship between water availability and grid operations as represented by a PCM for complementing existing regional and seasonal joint water–energy management planning. The fifth section of the supplement presents uncertainties in the estimate of the WSGIF and power operations under different sources of climate forcing and a different hydrology model.

We specifically explored August with the assumption that generation would be the largest constraint and not transmission. Results may vary for studies in June and July when operations should be more constrained by transmission capacities or other climate stressors. It may also further vary under climate change.

Climate variations associated with ENSO conditions and analyzed for application to hydrology studies often include precipitation, temperature, and storm tracks. Temperature trends tend to be more certain than precipitation trends. We analyzed here the sensitivity of power operations under water availability associated with ENSO conditions. The analysis could be complemented in the future with associated changes in temperatures, which would affect the agricultural water demand and the electricity demand. This is the subject of ongoing research.

The current modeling framework can be used to evaluate the performance of future grid infrastructures under evolving water availability conditions. Further understanding of how to cascade UCED operational constraints associated with water constrained hydropower generation and thermoelectric boundary conditions into grid expansion models, which do not consider the time-varying components of the constraints, is also the subject of ongoing research.

CONCLUSIONS. This paper provides benchmark characteristics for the electric power system in the western U.S. grid using 55 years of water-dependent boundary conditions in electricity generation that represent the historic variability of crucial water availability and their relevance to safe and reliable power supply. While interannual variability has been benchmarked for estimating the impacts on natural systems, the approach has never been applied to the electricity system. The value of establishing the baseline characteristics of grid operations with respect to long-term (55 years) water availability is that it can reveal potential vulnerabilities in the safe operation of large-scale regional electricity networks. This paper is the first to estimate 55 years of climate impacts on grid operations for the western U.S. grid. Time series of electricity grid operations metrics were derived for reliability (unserved energy, reserve margin) and economic perspective (production cost, carbon emission).

Using 55 years of historical hydroclimatology data with a 2010 level of water demand and water management infrastructure and a 2010 level of energy demand and power system infrastructure, August grid operations show a variation in production cost (–8% to +11%) and carbon emission (–7% to +11%). In terms of reliability, the capacity margin threshold is not reached; however, 5 out of the 55 years show unserved energy when no contingency plan is used. The benchmark provides a basis for climate change impact, vulnerability, and adaptation assessment because it provides a reference range of grid operations and guidance for grid expansion (e.g., risk assessment for sizing).

The study demonstrated the value of climate-related information to support power system operations and planning. For seasonal and multiyear planning (i.e., interannual and multiyear drought), ENSO climate oscillations indices can be used to plan for joint water–electricity management. In particular, El Niño conditions are less prone to brownout and power outages than neutral and La Niña conditions. Neutral ENSO conditions, however, tend to be associated with more economic power operations (–1%) over the WECC and less carbon emissions (–4%) in California. La Niña conditions are associated with the least economic operations (+5%) with the highest carbon emission in California (+5%), albeit the lowest in the PNW (–4%). PDO demonstrates the largest predictability but no resolution, while ENSO demonstrates smaller predictability but resolution in the projection of WSGIF and grid operations metrics. The benchmark provides a reference for seasonal operations in joint water–electricity management using a seasonal water availability outlook and climate oscillation for multiyear drought events.

The study complements existing assessments of the impact of climate variability and climate oscillations on regional water availability, with an application on the power system operations and planning sector. It highlights the need for further research in understanding and quantifying interregional water–energy dependencies. It also motivates the exploration of the sensitivity of specific grid operations (generation, transmission) to water availability and expands it to other climate-sensitive stressors like the electricity demand.

Future research toward improving the representation of nonstationary hydroclimate constraints, and opportunities, in UCED is needed to enhance the value of climate-related information toward more efficient and sustainable use of natural resources in power operations and more efficient and reliable power operations.

ACKNOWLEDGMENTS. This work was supported by the Office of Science of the U.S. Department of Energy, Office of Biological and Environmental Research, as part of the Integrated Assessment Research Program. We also acknowledge the World Climate Research Programme's Working Group on Coupled Modelling, which is responsible for CMIP, and we thank the National Center for Atmospheric Research (NCAR) for producing and making available their model output. For CMIP, the U.S. Department of Energy's Program for Climate Model Diagnosis and Intercomparison provided coordinating support and led development of software infrastructure in partnership with the Global Organization for Earth System Science Portals. The Pacific Northwest National Laboratory is operated by Battelle for the U.S. Department of Energy under Contract DE-AC05-76RL01830.

REFERENCES

Barnston, A. G., and C. F. Ropelewski, 1992: Prediction of ENSO episodes using canonical correlation analysis. *J. Climate*, **5**, 1316–1345, https://doi.org/10.1175/1520-0442(1992)005<1316:POEEUC>2.0.CO;2.

Bartos, M. D., and M. V. Chester, 2015: Impacts of climate change on electric power supply in the Western United States. *Nat. Climate Change*, **5**, 748–752, https://doi.org/10.1038/nclimate2648.

Biemans, H., I. Haddeland, P. Kabat, F. Ludwig, R. W. A. Hutjes, J. Heinke, W. von Bloh, and D. Gerten, 2011: Impact of reservoirs on river discharge and irrigation water supply during the 20th century. *Water Resour. Res.*, **47**, W03509, https://doi.org/10.1029/2009WR008929.

Boehlert, B., K. M. Strzepek, Y. Gebretsadik, R. Swanson, A. McCluskey, J. E. Neumann, J. McFarland, and J. Martinich, 2016: Climate change impacts and greenhouse gas mitigation effects on U.S. hydropower generation. *Appl. Energy*, **183**, 1511–1519, https://doi.org/10.1016/j.apenergy.2016.09.054.

Bureau of Reclamation, 2014: Downscaled CMIP3 and CMIP5 climate and hydrology projections: Release of hydrology projections, comparison with preceding information, and summary of user needs. U.S. Department of the Interior Bureau of Reclamation Rep., 110 pp.

——, 2016: SECURE Water Act section 9503(c)—reclamation climate change and water 2016. U.S. Department of the Interior Bureau of Reclamation Rep., 307 pp., www.usbr.gov/climate/secure/docs/2016secure/2016SECUREReport.pdf.

Cayan, D. R., M. D. Dettinger, R. T. Redmond, G. J. McCabe, N. Knowles, and D. H. Peterson, 2003: The transboundary setting of California's water and hydropower systems, linkages between the Sierra Nevada, Columbia, and Colorado hydroclimates. *Climate and Water: Transboundary Challenges in the Americas*, H. Diaz and B. Morehouse, Eds., Kluwer Press, 237–262.

Daly, C., M. Halbleib, J. I. Smith, W. P. Gibson, M. K. Doggett, G. H. Taylor, J. Curtis, and P. A. Pasteris, 2008: Physiographically-sensitive mapping of temperature and precipitation across the conterminous United States. *Int. J. Climatol.*, **28**, 2031–2064, https://doi.org/10.1002/joc.1688.

Davies, E., P. Kyle, and J. Edmonds, 2013: An integrated assessment of global and regional water demands for electricity generation to 2095. *Adv. Water Resour.*, **52**, 296–313, https://doi.org/10.1016/j.advwatres.2012.11.020.

DeNooyer, T. A., J. M. Peschel, Z. Zhang, and A. S. Stillwell, 2016: Integrating water resources and power generation: The energy–water nexus in Illinois. *Appl. Energy*, **162**, 363–371, https://doi.org/10.1016/j.apenergy.2015.10.071.

Dettinger, M. D., D. R. Cayan, H. F. Diaz, and D. M. Meko, 1998: North–south precipitation patterns in western North America on interannual-to-decadal timescales. *J. Climate*, **11**, 3095–3111, https://doi.org/10.1175/1520-0442(1998)011<3095:NSPPIW>2.0.CO;2.

Döll, P., K. Fiedler, and J. Zhang, 2009: Global-scale analysis of river flow alterations due to water withdrawals and reservoirs. *Hydrol. Earth Syst. Sci.*, **13**, 2413–2432, https://doi.org/10.5194/hess-13-2413-2009.

Feeley, T. J., T. J. Skone, G. J. Stiegel Jr., A. McNemar, M. Nemeth, B. Schimmoller, J. T. Murphy, and L. Manfredo, 2008: Water: A critical resource in the thermoelectric power industry. *Energy*, **33**, 1–11, https://doi.org/10.1016/j.energy.2007.08.007.

Hamlet, A. F., and D. P. Lettenmaier, 1999: Columbia River streamflow forecasting based on ENSO and PDO climate signals. *J. Water Resour. Plann.*

Manage., **125**, 333–341, https://doi.org/10.1061/(ASCE)0733-9496(1999)125:6(333).

Hanasaki, N., S. Kanae, and T. Oki, 2006: A reservoir operation scheme for global river routing models. *J. Hydrol.*, **327**, 22–41, https://doi.org/10.1016/j.jhydrol.2005.11.011.2006.

Harto, C. B., and E. Yan, 2011: Analysis of drought impacts on electricity production in the western and Texas interconnection. Argonne National Laboratory Rep. ANL/EVS/R-11/14, 161 pp.

Hejazi, M. I., J. Edmonds, V. Chaturvedi, E. Davies, and J. Eom, 2013: Scenarios of global municipal water use demand projections over the 21st century. *Hydrol. Sci. J.*, **58**, 519–538, https://doi.org/10.1080/02626667.2013.772301.

——, and Coauthors, 2014a: Long-term global water use projections using six socioeconomic scenarios in an integrated assessment modeling framework. *Technol. Forecasting Soc. Change*, **81**, 205–226, https://doi.org/10.1016/j.techfore.2013.05.006.

——, and Coauthors, 2014b: Integrated assessment of global water scarcity over the 21st century under multiple climate change mitigation policies. *Hydrol. Earth Syst. Sci.*, **18**, 2859–2883, https://doi.org/10.5194/hess-18-2859-2014.

——, and Coauthors, 2015: 21st century United States emissions mitigation could increase water stress more than the climate change it is mitigating. *Proc. Natl. Acad. Sci. USA*, **112**, 10 635–10 640, https://doi.org/10.1073/pnas.1421675112.

Kao, S.-C., M. J. Sale, M. Ashfaq, R. Uría Martínez, D. Kaiser, Y. Wei, and N. S. Diffenbaugh, 2015: Projecting changes in annual hydropower generation using regional runoff data: An assessment of the United States federal hydropower plants. *Energy*, **80**, 239–250, https://doi.org/10.1016/j.energy.2014.11.066.

Ke, X., D. Wu, J. S. Rice, M. C. W. Kintner-Meyer, and N. Lu, 2016: Quantifying impacts of heat waves on power grid operation. *Appl. Energy*, **183**, 504–512, https://doi.org/10.1016/j.apenergy.2016.08.188.

Kenny, J. F., N. L. Barber, S. S. Hutson, K. S. Linsey, J. K. Lovelace, and M. A. Maupin, 2009: Estimated use of water in the United States in 2005. U.S. Geological Survey Circular 1344, 52 pp.

Li, H., M. S. Wigmosta, H. Wu, M. Huang, Y. Ke, A. M. Coleman, and L. R. Leung, 2013: A physically based runoff routing model for land surface and Earth system models. *J. Hydrometeor.*, **14**, 808–828, https://doi.org/10.1175/JHM-D-12-015.1.

Liang, X., D. P. Lettenmaier, E. F. Wood, and S. J. Burges, 1994: A simple hydrologically based model of land surface water and energy fluxes for general circulation models. *J. Geophys. Res.*, **99**, 14 415–14 428, https://doi.org/10.1029/94JD00483.

Livneh, B., E. A. Rosenberg, C. Lin, B. Nijssen, V. Mishra, K. M. Andreadis, E. P. Maurer, and D. P. Lettenmaier, 2013: A long-term hydrologically based dataset of land surface fluxes and states for the conterminous United States: Update and extensions. *J. Climate*, **26**, 9384–9392, https://doi.org/10.1175/JCLI-D-12-00508.1.

Macknick, J., S. Sattler, K. Averyt, S. Clemmer, and J. Rogers, 2012: The water implications of generating electricity: Water use across the United States based on different electricity pathways through 2050. *Environ. Res. Lett.*, **7**, 045803, https://doi.org/10.1088/1748-9326/7/4/045803.

Mantua, N. J., S. R. Hare, J. M. Wallace, and R. C. Francis, 1997: A Pacific decadal climate oscillation with impacts on salmon production. *Bull. Amer. Meteor. Soc.*, **78**, 1069–1079, https://doi.org/10.1175/1520-0477(1997)078<1069:APICOW>2.0.CO;2.

Maurer, E. P., A. W. Wood, J. C. Adam, D. P. Lettenmaier, and B. Nijssen, 2002: A long-term hydrologically based data set of land surface fluxes and states for the conterminous United States. *J. Climate*, **15**, 3237–3251, https://doi.org/10.1175/1520-0442(2002)015<3237:ALTHBD>2.0.CO;2.

McKee, T. B., N. J. Doesken, and J. Kleist, 1993: The relationship of drought frequency and duration of time scales. *Eighth Conf. on Applied Climatology*, Anaheim, CA, Amer. Meteor. Soc., 179–186.

Palmer, W. C., 1965: Meteorological drought. U.S. Department of Commerce Weather Bureau Research Paper 45, 65 pp.

Poch, L. A., G. Conzelmann, and T. D. Veselka, 2009: An analysis of the effects of drought conditions on electric power generation in the western United States. National Energy Technology Laboratory Rep. DOE/NETL-2009/1365, 40 pp.

Redmond, K. T., and R. W. Koch, 1991: Surface climate and streamflow variability in the western United States and their relationship to large-scale circulation indices. *Water Resour. Res.*, **27**, 2381–2399, https://doi.org/10.1029/91WR00690.

Schaner, N., N. Voisin, B. Nijssen, and D. P. Lettenmaier, 2012: The contribution of glacier melt to streamflow. *Environ. Res. Lett.*, **7**, 034029, https://doi.org/10.1088/1748-9326/7/3/034029.

Scott, M. J., and Coauthors, 2016: Sensitivity of future U.S. water shortages to socioeconomic and climate drivers: A case study in Georgia using an integrated human-Earth system modeling framework. *Climatic Change*, **136**, 233–246, https://doi.org/10.1007/s10584-016-1602-8.

Sovacool, B. K., and K. E. Sovacool, 2009: Identifying future electricity–water tradeoffs in the United States. *Energy Pol.*, **37**, 2763–2773, https://doi.org/10.1016/j.enpol.2009.03.012.

Sheffield, J., and Coauthors, 2013: North American Climate in CMIP5 Experiments. Part I: Evaluation of historical simulations of continental and regional climatology. *J. Climate*, **26**, 9209–9245, https://doi.org/10.1175/JCLI-D-12-00592.1.

Taylor, K. E., R. J. Stouffer, and G. A. Meehl, 2012: An overview of CMIP5 and the experiment design. *Bull. Amer. Meteor. Soc.*, **93**, 485–498, https://doi.org/10.1175/BAMS-D-11-00094.1.

Tidwell, V. C., P. H. Kobos, L. A. Malczynski, G. Klise, and C. R. Castillo, 2012: Exploring the water-thermoelectric power nexus *J. Water Plann. Manage.*, **138**, 491–501, https://doi.org/10.1061/(ASCE)WR.1943-5452.0000222.

——, M. Bailey, K. M. Zemlick, and B. D. Moreland, 2016: Water supply as a constraint on transmission expansion planning in the Western interconnection. *Environ. Res. Lett.*, **11**, 124001, https://doi.org/10.1088/1748-9326/11/12/124001.

Trenberth, K. E., 1997: The definition of El Niño. *Bull. Amer. Meteor. Soc.*, **78**, 2771–2777, https://doi.org/10.1175/1520-0477(1997)078<2771:TDOENO>2.0.CO;2.

Union of Concerned Scientists, 2012: UCS EW3 energy-water database, version 1.3. Union of Concerned Scientists, accessed 11 November 2015, www.ucsusa.org/clean-energy/energy-water-use/ucs-power-plant-database.

Vano, J. A., M. Scott, N. Voisin, C. O. Stöckle, A. F. Halmet, K. E. B. Mickelson, M. M. Elsner, and D. P. Lettenmaier, 2010: Climate change impacts on water management and irrigated agriculture in the Yakima River basin, Washington, USA. *Climatic Change*, **102**, 287–317, https://doi.org/10.1007/s10584-010-9856-z.

Van Vliet, M. T. H., J. R. Yearsley, F. Ludwig, S. Vogele, D. P. Lettenmaier, and P. Kabat, 2012a: Vulnerability of US and European electricity supply to climate change. *Nat. Climate Change*, **2**, 676–681, https://doi.org/10.1038/nclimate1546.

——, ——, W. H. P. Franssen, F. Ludwig, I. Haddeland, D. P. Lettenmaier, and P. Kabat, 2012b: Coupled daily streamflow and water temperature modelling in large river basins. *Hydrol. Earth Syst. Sci.*, **16**, 4303–4321, https://doi.org/10.5194/hess-16-4303-2012.

——, D. Wiberg, S. Leduc, and K. Riahi, 2016: Power-generation system vulnerability and adaptation to changes in climate and water resources. *Nat. Climate Change*, **6**, 375–380, https://doi.org/10.1038/nclimate2903.

Vicente-Serrano, S., J. López-Moreno, S. Beguería, J. Lorenzo-Lacruz, C. Azorin-Molina, and E. Morán-Tejeda, 2012: Accurate computation of a streamflow drought index. *J. Hydrol. Eng.*, **17**, 318–332, https://doi.org/10.1061/(ASCE)HE.1943-5584.0000433.

Voisin, N., A. F. Hamlet, L. P. Graham, D. W. Pierce, T. P. Barnett, and D. P. Lettenmaier, 2006: The role of climate forecasts in western U.S. power planning. *J. Appl. Meteor. Climatol.*, **45**, 653–673, https://doi.org/10.1175/JAM2361.1.

——, H. Li, D. Ward, M. Huang, M. Wigmosta, and L. R. Leung, 2013a: On an improved sub-regional water resources management representation for integration into Earth system models. *Hydrol. Earth Syst. Sci.*, **17**, 3605–3622, https://doi.org/10.5194/hess-17-3605-2013.

——, L. Liu, M. Hejazi, T. Tesfa, H. Li, M. Huang, Y. Liu, and L. R. Leung, 2013b: One-way coupling of an integrated assessment model and a water resources model: Evaluation and implications of future changes over the US Midwest. *Hydrol. Earth Syst. Sci.*, **17**, 4555–4575, https://doi.org/10.5194/hess-17-4555-2013.

——, M. Kintner-Meyer, J. Dirks, R. Skaggs, D. Wu, T. Nguyen, Y. Xie, and M. Hejazi, 2016: Vulnerability of the US western electric grid to hydro-climatological conditions: How bad can it get? *Energy*, **115**, 1–12, https://doi.org/10.1016/j.energy.2016.08.059.

Wang, S., J. Huang, Y. He, and Y. Guan, 2014: Combined effects of the Pacific decadal oscillation and El Niño–Southern Oscillation on global land dry–wet changes. *Sci. Rep.*, **4**, 6651, https://doi.org/10.1038/srep06651.

Zagona, E. A., T. J. Fulp, R. Shane, T. Magee, and H. M. Goranflo, 2001: Riverware: A generalized tool for complex reservoir system modeling. *J. Amer. Water Resour. Assoc.*, **37**, 913–929, https://doi.org/10.1111/j.1752-1688.2001.tb05522.x.